Using a piezoelectric fiber stretcher to remove the depth ambiguity in Optical Fourier Domain Imaging

Vergnole, Sébastien; Lamouche, Guy; Dufour, Marc; Gauthier, Bruno

Publisher's version / Version de l'éditeur:

Proceedings of the European Conferences on Biomedical Optics 2007, 2007-06-18

Using a piezoelectric fiber stretcher to remove the depth ambiguity in Optical Fourier Domain Imaging

Sébastien Vergnole, Guy Lamouche, Marc Dufour and Bruno Gauthier

Industrial Materials Institute, National Research Council,

75 bd de Mortagne, Boucherville, QC, Canada

ABSTRACT

This paper reports the study of an Optical Fourier Domain Imaging (OFDI) setup for optical coherence tomography. One of the main drawbacks of OFDI is its inability to differentiate positive and negative depths. Some setups have already been proposed to remove this depth ambiguity by introducing a modulation by means of electro-optic or acousto-optic modulators. In our setup, we implement a piezoelectric fiber stretcher to generate a periodic phase shift between successive A-scans, thus introducing a transverse modulation. The depth ambiguity is then resolved by performing a Fourier treatment in the transverse direction before processing the data in the axial direction. It is similar to the B-M mode scanning already proposed for Spectral-Domain OCT[1] but with a more efficient experimental setup. We discuss the advantages and the drawbacks of our technique compared to the technique based on acousto-optics modulators by comparing images of an onion obtained with both techniques.

Keywords: Optical Fourier Domain Imaging, Depth Ambiguity, Piezoelectric Fiber Stretcher

1. INTRODUCTION

In Fourier-Domain OCT (FD-OCT), the signal is collected as a function of the wavelength and the spatial information is recovered by Fourier transform. Two kinds of setups can be used. The first one is called Spectral-Domain OCT (SD-OCT) and uses a broadband source while relying on detection with a spectrometer to separate the spectral components.[2,3] The second one is Optical Fourier Domain Imaging (OFDI)[4] also known as Swept Source OCT (SS-OCT). In this case, the spectral components are separated at launch with a wavelength-swept source. In both cases, the main drawback is that, since it is a real signal that is acquired, the Fourier transform is symmetric around the origin. Therefore, one cannot distinguish the positive depth from the negative depth. Additionally, autocorrelation terms in the recording signal lead to a spurious component at zero frequency (DC artefact). For OFDI, some setups have already been proposed to remove this depth ambiguity by shifting the frequency by means of electro-optic[5] or acousto-optic modulators.[6,7] In SD-OCT, one solution that uses B-M scanning with a mirror mounted on a piezoelectric transducer has been proposed by Yasuno et al.[1] A phase shift is introduced between consecutive A-scans to generate a transverse modulation that is used to remove both the depth degeneracy and the DC artefact. In Ref. 1 the experimental setup does not allow discrete increments in phase shift. Consequently, a triangular ramp is used that generates other artifacts that require further data processing to be removed.

Here, we implement B-M type scanning with a piezoelectric fiber stretcher in our OFDI setup. This is the first reported demonstration of B-M scanning for an OFDI system. The use of a fiber stretcher improves over Ref. 1 by allowing the fast generation of discrete steps in the phase shift generated between A-scans. This avoids the introduction of additional artifacts and leads to a more efficient technique.

The next section is dedicated to our experimental setup. Then, the signal processing technique is described showing examples on different samples. Finally, we also present the advantages and drawbacks of such a technique compared to the technique using acousto-optics modulators.

Further author information: (Send correspondence to S.V.)
S.V.: E-mail: Sebastien.Vergnole@cnrc-nrc.gc.ca, Telephone: +1 450 641 5137

2. EXPERIMENTAL SETUP

Fourier-Domain OCT has concentrated a lot of researchers' efforts in recent years. The two main advantages of this technique is that there is no moving part in the reference arm and that it provides a better signal-to-noise ratio than Time-Domain OCT.[8] As written in the introduction, two kinds of setups may be used in FD-OCT. In our institute, this is an OFDI setup which is used (see Fig. 1).

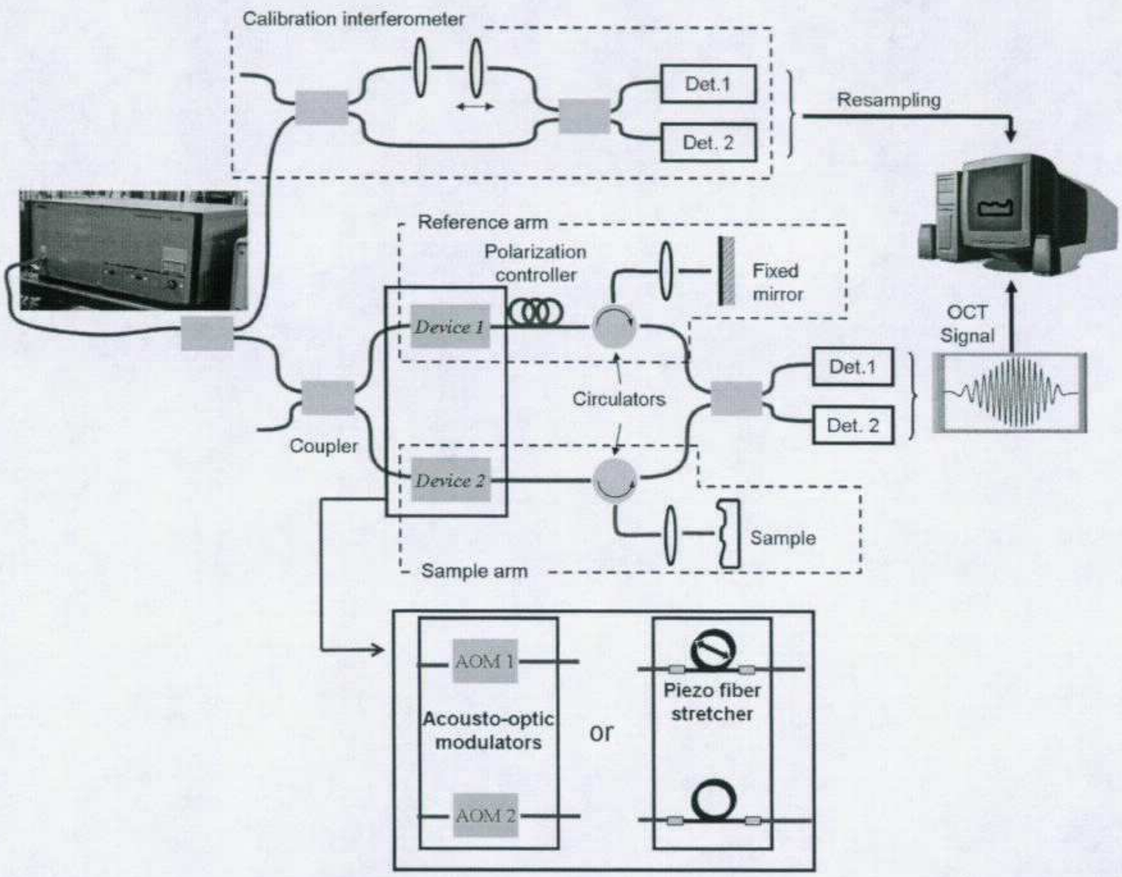

Figure 1. IMI Optical Fourier Domain Imaging setup. Devices 1 and 2 are replaced either by AOMs or PFS.

More precisely, it is a Mach-Zehnder fiber-based interferometer. The source is a Thorlabs swept-source with a 1325 nm center wavelength and a 85 nm FWHM. The theoretical axial resolution is $\delta z = 9.1$ μm in air. The A-scan rate is 16 kHz when using both the backward and the forward wavelength scans. The setup can either be fitted with acousto-optic modulators (AOMs) or with a piezoelectric fiber stretcher (PFS). The AOMs used in our setup are bulk AOMs from IntraAction. The frequency of the first one is 70 MHz whereas for the second one the frequency is 80 MHz which yields to a 10 MHz frequency shift between the two arms of the interferometer. This frequency shift allows us to remove the depth ambiguity as it was shown in Yun et al.[6] and Davis et al.[7] The PFS is from Optiphase (*PZ1-STD-FC/APC*). Around 10 m of fiber are wound around a cylindrical piezo-electric transducer. Figure 2 gives the shape of the low voltage applied to the PFS. The PFS drive voltage is adjusted to achieved a $\pi/2$ phase shift between two consecutive forward wavelength scan interferograms. The system operates at a reduced rate of 8 kHz since we only use the forward wavelength scans.

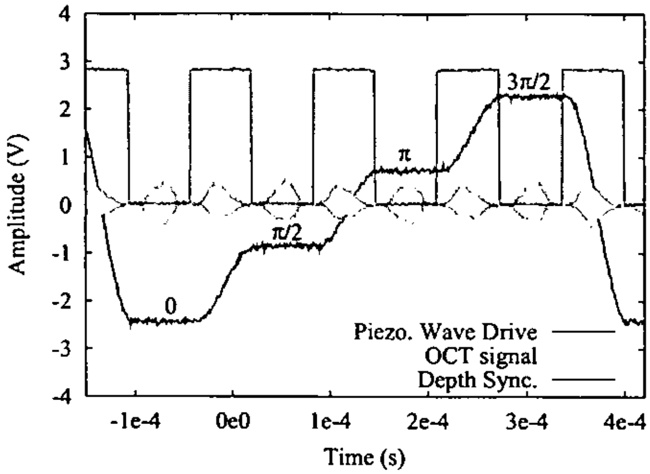

Figure 2. Red: PFS Drive Wave, Green: OCT signal, Black: Depth synchronization. The PFS drive wave is synchronized with the depth sync. signal. Each step of the PFS drive wave happens for a forward wavelength scan.

3. SIGNAL PROCESSING

3.1. Theory

The signal processing is basically the same as the one used in Yasuno et al.[1] It has some similarity with phase shifting interferometry. It can be illustrated with the simple case of a single reflector. For a B-scan, a simplified version of the interferometric signal is:

$$i(x,\nu) = k_0 + \cos(k_x x + k_\nu \nu) \tag{1}$$

where k_0 is a constant that includes the autocorrelation terms, k_x is linked with the phase shift introduced by the PFS, x is the transverse position, k_ν is linked with the wavelength sweeping of the source and ν is the optical frequency.

We, first, compute the transverse Fourier transform (along x):

$$I(u,\nu) = \mathcal{F}_x[i(x,\nu)] = k_0\delta(u) + \frac{1}{2}\cdot\delta(u-k_x)\cdot\exp(-ik_\nu\nu) + \frac{1}{2}\cdot\delta(u+k_x)\cdot\exp(ik_\nu\nu) \tag{2}$$

where u is the Fourier conjugate of x, $k_0\delta(u)$ is the DC component, the second term on the right hand side is the OCT data, and the last term is the complex conjugate of the second one.
A high-pass filtering with a rectangular window is then performed to keep only the data corresponding to the OCT signal to yield:

$$\hat{I}(u,\nu) = \frac{1}{2}\cdot\delta(u-k_x)\cdot\exp(-ik_\nu\nu) \tag{3}$$

Then, we compute the inverse transverse Fourier transform

$$\hat{i}(x,\nu) = \mathcal{F}_x^{-1}\left[\hat{I}(u,\nu)\right] = \frac{1}{2}\cdot\exp(-ik_x x)\cdot\exp(-ik_\nu\nu) \tag{4}$$

Finally, the axial Inverse Fourier transform is evaluated:

$$\hat{I}(x,z) = \mathcal{F}_z^{-1}\left[\hat{i}(x,\nu)\right] = \frac{1}{2}\cdot\exp(-ik_x x)\cdot\delta(z-k_\nu) \tag{5}$$

where z is the Fourier conjugate of ν and corresponds to the depth position. To obtain the OCT image, we keep the amplitude of the complex number $\hat{I}(x,z)$ obtained in equation 5.

3.2. Example with a fixed mirror as a sample

Figure 3 provides an example of signal processing for measurements performed on a fixed sample. In this case, 2048 A-scans of 1024 points were acquired at the same point (i.e. without transverse motion of the optical probe), with a $\pi/2$ phase shift introduced between successive A-scans.

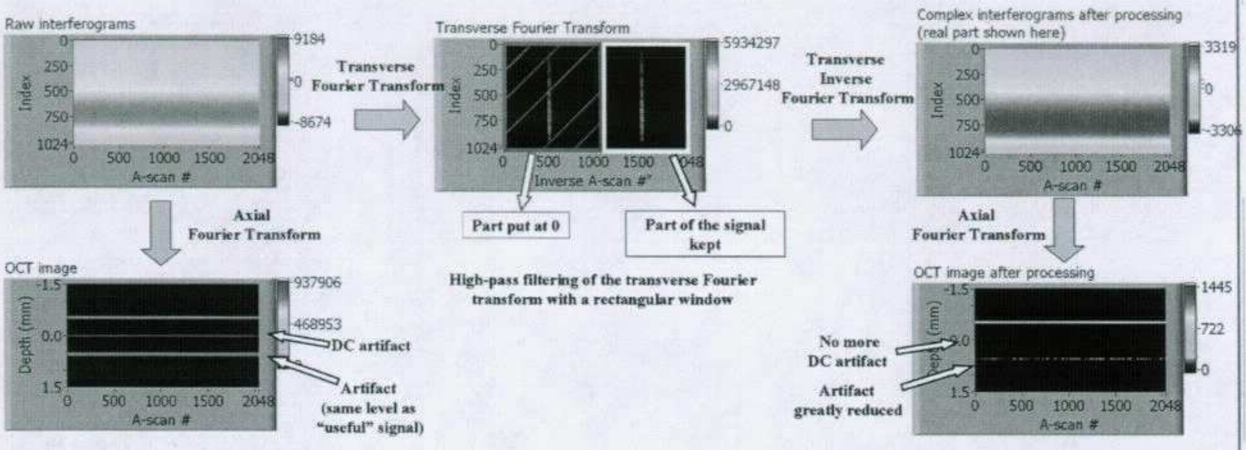

Figure 3. Example of signal processing for a fixed mirror as a sample

It shows that this technique enables to remove the DC artifact and to greatly reduce the mirror image.

3.3. Evolution of the artifact removal as a function of the transverse step

The transverse step must be carefully chosen in order to provide an efficient removal of the mirror image artifact. Figure 4 shows images of an onion obtained with transverse steps from 0.6 μm to 6.4 μm. The sample is placed below the zero delay position in order to evaluate how the mirror image is attenuated.

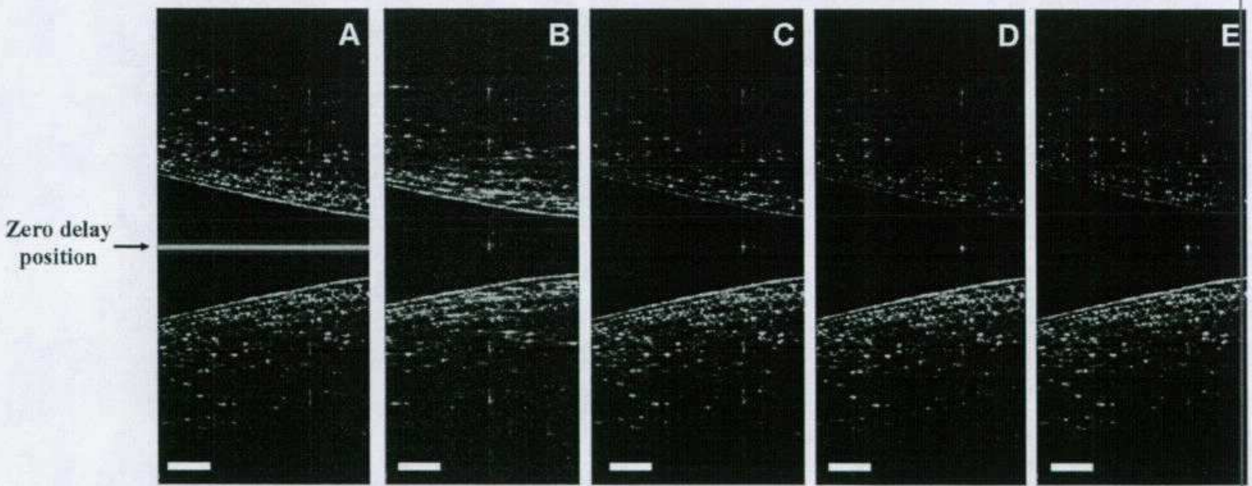

Figure 4. Effect of the transverse step. Extreme left (A): step of 0.6 μm, no processing. Then from left to right , the transverse step decreases (6.4 μm (B), 2.5 μm (C), 1.3 μm (D) and 0.6 μm (E)) and we process our data with the algorithm described above. Images are 2.5 cm wide and 6 mm depth. The horizontal white line at the bottom left of each image is 500 μm.

The efficiency of mirror artifact removal increases as the transverse step is decreased. The small transverse step ensures that only small changes occur between two consecutive A-scans.

4. COMPARISON

In order to compare the efficiency of our PFS system with that of the existing AOM system, we present images of an onion obtained with the two setups. The transverse step is 0.6 μm in both cases. Figure 5 shows the image acquired with the AOMs setup. The frequency shift introduced by the AOMs enables to shift the zero path delay. Thus, the zero position no longer corresponds to the zero frequency and we can differentiate the negative from the positive depths. It may be seen on the right that the mirror image and DC artifact are completely removed.

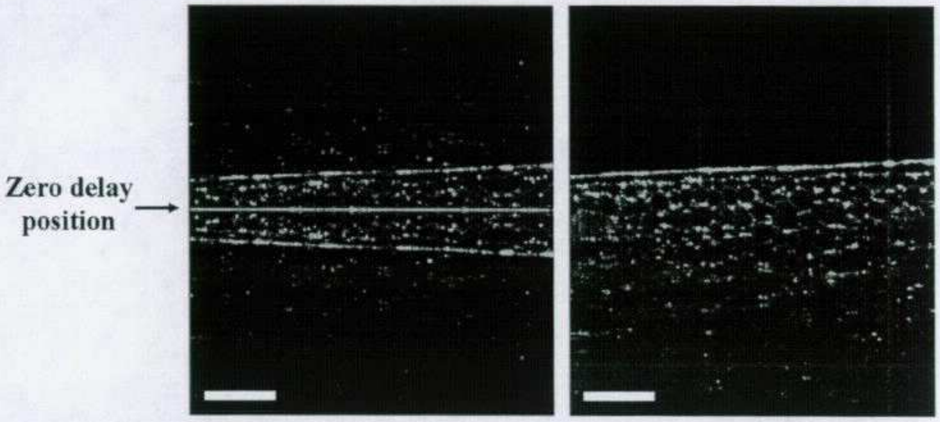

Figure 5. Images of an onion with the AOM setup. Left: image with artifacts. Right: artifacts removed. Images are 2.5 mm wide and 3 mm depth. The horizontal white line at the bottom left of each image is 500 μm.

Figure 6 shows the onion image obtained with the PFS setup before and after signal processing. Here the DC artifact is completely removed and the mirror image is greatly reduced. The cells of the onion can be as clearly seen as with the AOM setup.

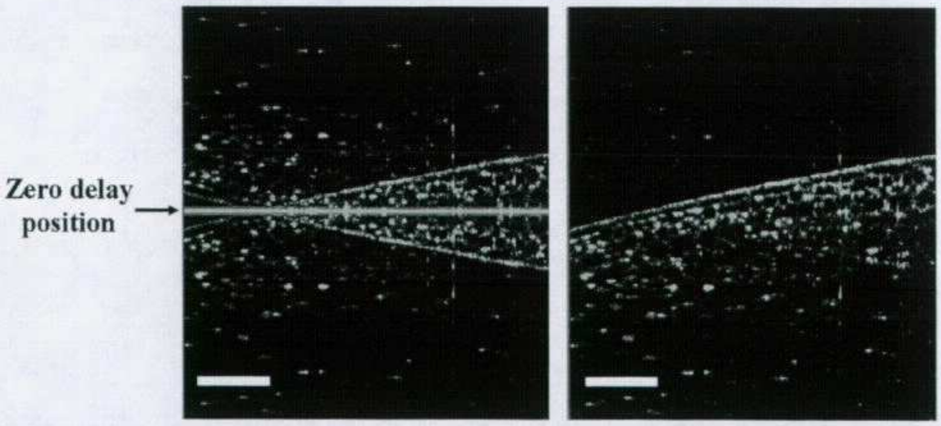

Figure 6. Images of an onion with the PFS setup. Left: raw data without processing. Right: with processing. Images are 2.5 mm wide and 3 mm depth. The horizontal white line at the bottom left of each image is 500 μm.

Table 1 shows the advantages and the drawbacks of using a PFS setup compared to an AOM setup.

Table 1. Advantages and drawbacks of using the piezolectric fiber stretcher compared to acousto-optic modulators

Advantages	Drawbacks
• All-guided interferometer: very easy to align and low power loss • Low cost (500 \$ vs 10000 \$) • Compact (5 × 5 cm vs 30 × 40 cm, see photo on figure 7) • Does not affect the measurement nor request a change of setup when not in use	• Increased post-processing (time and complexity) • Mirror artifact not completely removed • Small transverse steps needed (lower scan speed)

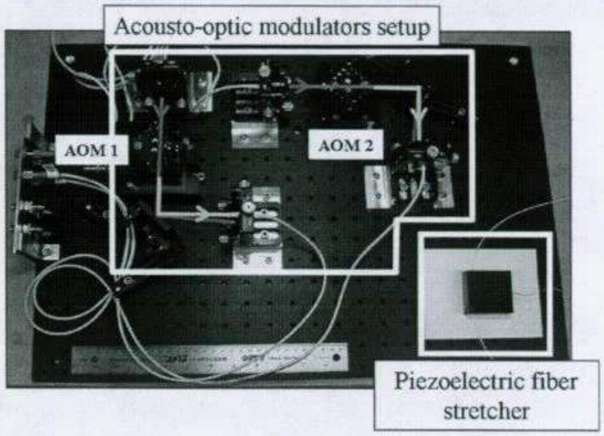

Figure 7. Setup photo: comparison of the AOM setup and the piezoelectric PFS to illustrate the compactness of the PSF versus AOMs

5. CONCLUSION

To conclude, we can say that an implementation of a B-M type scanning with a piezoelectric fiber stretcher in an OFDI setup provides images with greatly reduced artifacts. It is the first time to our knowledge that a B-M-mode scanning with a piezoelectric fiber stretcher has been reported in OFDI or SS-OCT. This technique has three main advantages over the setup using bulk AOMs. Firstly, it is very easy to implement experimentally because the PFS is a fiber-based device with FC-APC connectors. It is not only easy to insert in the setup but it is also very efficient in terms of power transmission since the only small losses are due to the fiber connections. Secondly, it is low cost. Thirdly, it is very compact, occupying a surface of about 25 cm^2. Thus, this B-M-mode scanning technique with a PSF is a very promising approach to remove depth degeneracy in OFDI or SS-OCT.

ACKNOWLEDGMENTS

We acknowledge the financial support of the Genomics and Health Initiative of the National Research Council Canada.

REFERENCES

1. Y. Yasuno, S. Makita, T. Endo, G. Aoki, M. Itoh, and T. Yatagai, "Simultaneous b-m-mode scanning method for real-time full-range fourier domain optical coherence tomography," *Applied Optics* **45**(8), pp. 1861–1865, 2006.
2. A. F. Fercher, C. K. Hitzenberger, G. Kamp, and S. Y. El Zaiat, "Measurement of intraocular distances by backscattering spectral interferometry," *Optics Communications* **117**(1-2), pp. 43–48, 1995.

3. G. Hausler and M. W. Linduer, ""coherence radar" and "spectral radar"-new tools for dermatological diagnosis," *Journal of Biomedical Optics* **3**(1), pp. 21–31, 1998.
4. S. H. Yun, G. J. Tearney, J. F. de Boer, N. Iftimia, and B. E. Bouma, "High-speed optical frequency-domain imaging," *Optics Express* **11**(22), pp. 2953 – 2963, 2003.
5. J. Zhang, J. S. Nelson, and Z. Chen, "Removal of a mirror image and enhancement of the signal-to-noise ratio in fourier-domain optical coherence tomography using an electro-optic phase modulator," *Optics Letters* **30**(2), pp. 147–149, 2005.
6. S. H. Yun, G. J. Tearney, J. F. de Boer, and B. E. Bouma, "Removing the depth-degeneracy in optical frequency domain imaging with frequency shifting," *Optics Express* **12**(20), pp. 4822 – 4828, 2004.
7. A. M. Davis, M. A. Choma, and J. A. Izatt, "Heterodyne swept-source optical coherence tomography for complete complex conjugate ambiguity removal," *Journal of Biomedical Optics* **10**(6), pp. 064005–1 – 064005–6, 2005.
8. M. A. Choma, M. V. Sarunic, C. Yang, and J. A. Izatt, "Sensitivity advantage of swept source and fourier domain optical coherence tomography," *Optics Express* **11**(18), pp. 2183 – 2189, 2003.